MONITORING DYNAMIC DEFORMATION OF SHUTTLE STEEL SHELVES BY DIGITAL PHOTOGRAPHY

Chengxin Yu[1], Guojian Zhang[2], Xinhua Ding[3], Yongqian Zhao[4] and Guangli Guo[5]

1. *Business School, Shandong Jianzhu University, Fengming Road 1000, 250101 Jinan, Shandong, China; ycx1108@126.com (Corresponding author)*
2. *NASG Key Laboratory of Land Environment and Disaster Monitoring & School of Environmental Science and Spatial Informatics, China University of Mining and Technology, Daxue Road 1, 221116 Xuzhou, Jiangsu, China; g_j_zhang@cumt.edu.cn*
3. *Map Institute of Shandong Province, Jinan, Shandong; 250001, China, email: ding_xin_hua@126.com*
4. *School of Science, Shandong Jianzhu University, Fengming Road 1000, 250101 Jinan, Shandong, China; Yongqian_Zhao@126.com*
5. *NASG Key Laboratory of Land Environment and Disaster Monitoring & School of Environmental Science and Spatial Informatics, China University of Mining and Technology, Daxue Road 1, 221116 Xuzhou, Jiangsu, China; guo_gli@126.com*

ABSTRACT

Shuttle steel shelves (steel shelves equipped with shuttles) are popular in modern logistics. The safety of shuttle steel shelves is an issue due to the complicated dynamic load that develops when the shuttles are in operation. As deformation is an important index of structural safety, this study uses a DPS (digital photography system) based on the PST-IM-MP (photograph scale transformation-image matching-motion parallax) method to monitor shuttle steel shelves: a digital camera (SONY350) was used to monitor the dynamic deformation of shuttle steel shelves when the shuttles began to move, accelerated, moved at constant speed, decelerated and stopped. Then, the deformation trends of the shuttle steel shelves were depicted to study the moving trajectory in a local area. Moreover, we analysed the stresses in the shuttle steel shelves based on these monitoring data. The results showed that the PST-IM-MP method can meet the accuracy requirements in monitoring the dynamic deformation of steel shelves as the maximum and minimum measurement errors were 0.74 pixels and 0.34 pixels in the comprehensive direction, respectively. The shuttle steel shelves were robust because the deformations were elastic and within the allowed10mm. Shear and tension stresses developed in the shuttle steel shelves when the shuttles were in operation. Thus, in the future DPS will become popular for monitoring shuttle steel shelves in real time to warn of possible dangers and mitigate hazards. Additionally, the monitoring data can be used to study the stability of the shuttle steel shelves to improve the related stability design theory.

KEYWORDS

DPS (digital photography system), Shuttle steel shelf, Dynamic deformation, Safety monitoring, PST-IM-MP (photograph scale transformation-image matching-motion parallax) method

INTRODUCTION

As the logistics business grows with the development of society, logistics systems become increasingly important. Warehouse shelves are indispensable equipment for logistics systems and the premise to the normal operation of the logistics systems [1]. Steel shelves are widely used in the storage of warehouse goods due to the high strength, light weight, good ductility and strong earthquake resistance of these shelves. The safety associated with steel shelves is an outstanding problem. Although scholars have studied the stabilities of steel shelf components (shelf columns [2], shelf beams [3] and shelf nodes [4]) and the stabilities of shelves overall [5] by theoretical analyses, structural tests and numerical simulations, and the rich research results have improved the stability design of steel shelf [6]. However, many accidents still occur during the use of steel shelf, especially shuttle steel shelves. The dynamic influences of shuttle operation cause certain areas to develop large wobbles and deformation, which makes traditional steel shelf design theory unable to meet the safety design requirements of shuttle steel shelves [7,8]. Thus, the safety of shuttle steel shelves is an urgent issue that needs to be addressed. Considering that deformation is an important index of structural safety, monitoring the dynamic deformation of shuttle steel shelves in operation is an important way to study this safety problem.

Traditional surveying methods such as use of the level instruments and the total stations can measure the static deformation of a target with high precision but cannot monitor the dynamic deformation over time. Such a task is technically possible for a physical sensor but is practically challenging due to the limited application of physical sensors for local deformation and the vulnerability of sensors in direct contact with the target. GPS (global positioning system) has proved effective in monitoring dynamic deformation [9]. However, the use of this method is restricted indoors because GPS cannot always receive a satellite signal. Although three-dimensional laser scanning has high measurement accuracy in monitoring the global deformation of a static object, this method cannot capture instantaneous dynamic deformation [10]. Digital photography is a non-contact measurement technique that continuously uses a non-metric digital camera to photograph an object to record its global and local dynamic deformation of the object over time.

Digital photography has been used to monitor the dynamic deformation of engineering structures such as masonry walls [11], bridge structures [12] and steel structures [13]. Certain researchers used digital photography to monitor the vibration deformation of steel shelves [1]. These examples suggest that using digital photography is feasible for monitoring dynamic deformation of shuttle steel shelves to study the safety issues when the shuttles are in operation.

The aim of this study is to use digital photography to monitor dynamic deformation of shuttle steel shelves over time when the shuttles are in operation. Real-time deformation trends depicted by a DPS (digital photography system) are used to assess the safety of shelves on site and to give timely warning of possible dangers. Moreover, the monitoring data is provided to facilitate the study of the stability of shuttle steel shelves to improve the design theory of these shelves.

DOI 10.14311/CEJ.2019.02.0012

DIGITAL PHOTOGRAPHY SYSTEM

The DPS (digital photography system) consists of hardware (a SONY350 camera and a computer) and software (data processing software for steel shelves). The key techniques of the DPS are detailed in the following sections.

Accuracy assessment of the digital camera

A Sony350 camera is used in this study. The view and parameters of the camera are showed in Figure 1 and Table 1, respectively. The distortion of the camera in the photographic system plays a major role in the measurement accuracy [14]. Assuming that the digital camera and the object do not move during testing, research shows that the distortion errors are linear near the centers of the resulting images. Thus, we adopt a grid method in the study to eliminate the distortion of the digital camera [15].

(a) *(b)* *(c)*

Fig.1 - Images of the Sony350 camera

Tab. 1 - Parameters of the Sony-350 camera

Type	Ser	Sensor sc	Focal lengt	Active pixels
Sony DSLR A350 (Sony-350)	C(	23.5×15.7	35mm (27-3	4592×3056 pixe

After correcting the distortion, we used the direct linear transformation (DLT) method [16,17] to assess the measurement accuracy of the digital camera:

(1) the forward: we use the spatial and pixel coordinates of reference points C_0-C_7 (in Table 2 of [18]) to solve for the coefficient between the spatial coordinates and pixel coordinates of the points in the photo;

(2) the inversion: we use the coefficient between the spatial coordinates and pixel coordinates of the points (in Table 3 of [18]) in the photo and the pixel coordinates of the points on the photographs to be solved for determining the spatial coordinates. Note that at least two photographs from different positions had to be taken to compute spatial coordinates for accuracy test.

Based on the relative data (in Table 2) and Equation (1), we obtain the measurement accuracy (in Table 3) of the digital camera:

$$\delta = \sqrt{\frac{[\Delta\Delta]}{n}} \quad (1)$$

where Δ is the true error, n is the number of true errors, and δ is the mean squared error.

In Table 3, the mean squared error of the Sony350 camera is 0.58mm. This result suggests that the camera used in this study meets the accuracy requirements for deformation observation. In Table 2, L represents the differences between the actual coordinates and the calculated coordinates of the deformation points. In Table 3, E (L) represents the mathematically expected value of L, and Δ is equal to E (L) minus L. Leica TM30 measurement robot was used to monitor 3D-coordinates of the necessary points. The angular accuracy and ranging accuracy of Leica TM30 are 0.5 seconds and 0.6mm+1ppm, respectively. In the test, the ranging accuracy of this measurement robot is approximately 0.6mm because the measuring distance is short.

Tab. 2- Spatial coordinates of deformation points U0 and U1

Name	Actual coordinates/r	Calculated coordinates/r	Differences(L)/mm
U0-X	108.8250	108.8260	1.0
U0-Y	95.8870	95.8880	1.0
U0-Z	99.4410	99.4400	1.0
U1-X	109.0670	109.0650	2.0
U1-Y	96.9350	96.9340	1.0
U1-Z	99.3940	99.3940	0.0

Tab. 3- Accuracy assessments of the digital camera/mm

L	1.0	1.0	1.0	2.0	1.0	0.0
E (L)	1.0					
Δ	0.0	0.0	0.0	-1.0	0.0	1.0
δ	0.58					

Photograph scale transformation-motion parallax method

The motion parallax method uses a camera to photograph an object before and after deformation to obtain the zero and successive images. The camera is in the same position and the optical axis of the camera is perpendicular to the object during measurement. The zero and successive images should be obtained with the same internal and external orientation elements. However, the internal and external orientation elements are always changing during the measurement process. Sometimes we cannot ignore the influence of this phenomenon on the coordinates of the image points. Then, the image matching-motion parallax (IM-MP) method is used to correct the influence of this phenomenon on the measurement results and to improve the measurement accuracy. However, sometimes the reference points and the deformation points are not on the same plane. Thus, this paper provides the photograph scale transformation-image matching-motion parallax method (PST-IM-MP) method to solve this problem.

In Figure 2 (a), we assume that point a (x_1^d, z_1^d) and point b (x_2^d, z_2^d) are the coordinates of the same deformation point on the zero and successive images, respectively. (dx_1^d, dz_1^d) and (dx_2^d, dz_2^d) are the systematic errors of the corresponding deformation point on the zero and

successive images, respectively. $(\Delta p_x^d, \Delta p_z^d)$ are the parallaxes of the deformation point on the image plane. Equation (2) can be expressed as:

$$\left.\begin{aligned}(x_2^d - x_1^d) - (dx_2^d - dx_1^d) - \Delta p_x^d = 0\\ (z_2^d - z_1^d) - (dz_2^d - dz_1^d) - \Delta p_z^d = 0\end{aligned}\right\} \quad (2)$$

On the object plane, Δx^d and Δz^d of the corresponding deformation point are:

$$\left.\begin{aligned}\Delta x^d = m \cdot \Delta p_x^d\\ \Delta z^d = m \cdot \Delta p_z^d\end{aligned}\right\} \quad (3)$$

where m is the photograph scale on the reference plane and Δx^d and Δz^d are the horizontal and vertical deformations of the deformation point on the object plane. Δp_x^d and Δp_z^d are the horizontal and vertical parallaxes of the corresponding image point on the image plane. Note that there are systematic errors in Δp_x^d and Δp_z^d .

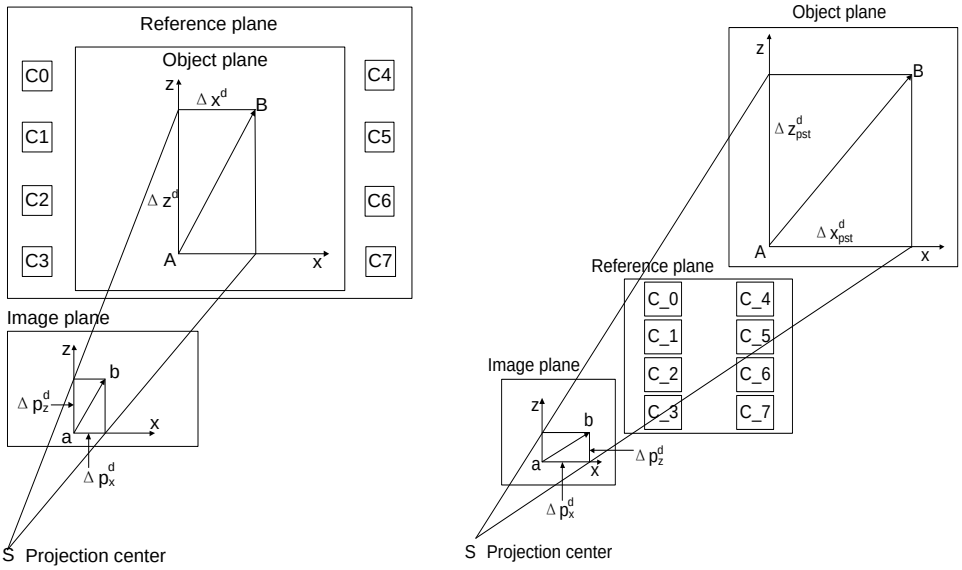

(a) Principle of the IM-MP method (b) Principle of the PST-IM-MP method

Fig. 2 - Principles of image matching- time baseline parallax

For the reference points, Equation (2) can be expressed as：

$$\left.\begin{aligned}(x_2^r - x_1^r) - (dx_2^r - dx_1^r) = 0\\ (z_2^r - z_1^r) - (dz_2^r - dz_1^r) = 0\end{aligned}\right\} \quad (4)$$

where (x_1^r, z_1^r) and (x_2^r, z_2^r) are the coordinates of the same reference point on the zero and successive images, respectively. (dx_1^r, dz_1^r) and (dx_2^r, dz_2^r) are systematic errors of the corresponding reference point on the zero and successive images, respectively.

Δp_x^r [17] is the parallax of the reference point, and the equation for this term can be expressed as:

$$\left.\begin{aligned} \Delta p_x^r &= (x_2^r - x_1^r) = (dx_2^r - dx_1^r) = \Delta p_x^{r0} + \delta p_x^r \\ \Delta p_x^{r0} &= (-\frac{\Delta Z_S}{Z} - \frac{\Delta f}{f})x_1^r + \Delta\kappa z_1^r + (-\frac{f}{Z}\Delta X_S - f\Delta\varphi - \Delta x_0) - \frac{x_1^{r2}}{f}\Delta\varphi - \frac{x_1^r z_1^r}{f}\Delta\omega \\ \delta p_x^r &= -(\frac{\Delta p_x^r dZ_{S2}}{Z}) - \frac{2\Delta p_x^r x_1^r}{f}d\varphi_2 - \frac{\Delta p_x^r z_1^r}{f}d\omega_2 - \frac{\Delta p_z^r x_1^r}{f}d\omega_2 + \Delta p_z^r d\kappa_2 - \frac{df_2}{f}\Delta p_z^r \end{aligned}\right\} \quad (5)$$

where $(X_S, Z_S, \varphi, \omega, \kappa, f, x_0)$ are the internal and external orientation elements of the zero and successive images and $(\Delta X_S, \Delta Z_S, \Delta\varphi, \Delta\omega, \Delta\kappa, \Delta f, \Delta x_0)$ are the changes in the internal and external orientation elements of the successive image relative to the zero image. Δp_x^{r0} is the function of the reference point coordinates on the image plane, $(dZ_{S2}, d\varphi_2, d\omega_2, d\kappa_2, df_2)$ are the internal and external orientation elements of the successive image themselves, $(\Delta p_x^r, \Delta p_z^r)$ are the parallax of reference points on the image plane, and δp_x^r is the parallax caused by the errors of the internal and external orientation elements of the images themselves and $(\Delta p_x^r, \Delta p_z^r)$.

Δp_x^{r0} can also be expressed as Equation (6):

$$\Delta p_x^{r0} = a_x x^r + b_x z^r + c_x + d_x x^{r2} + e_x x^r z^r \quad (6)$$

where $a_x = -\frac{\Delta Z_S}{Z} - \frac{\Delta f}{f}$, $b_x = \Delta\kappa$, $c_x = -\frac{f}{Z}\Delta X_S - f\Delta\varphi - \Delta x_0$, $d_x = -\frac{\Delta\varphi}{f}$, $d_x = -\frac{\Delta\omega}{f}$, (a_x, b_x) and (a_z, b_z) are the parallax coefficients in the X- and Z-direction respectively, (c_x, d_x) are the constant parallax coefficients in the X- and Z-direction respectively, and (x^r, z^r) are the coordinates of the reference points on the image plane.

As $(\Delta p_x^{r0}, \Delta p_z^{r0})$ are tiny amounts, their quadratic terms are negligible, and Equation (7) is obtained:

$$\left.\begin{aligned} \Delta p_x^{r0} &= a_x x^r + b_x z^r + c_x \\ \Delta p_z^{r0} &= a_z x^r + b_z z^r + c_z \end{aligned}\right\} \quad (7)$$

In this case, we only need three or more reference points to obtain (a_x, b_x, c_x) and (a_z, b_z, c_z). After barycentralizing the image point coordinates, we obtain the coordinates $(x^r{}', z^r{}')$ and the systematic error $(\Delta p_x^{r0}{}', \Delta p_z^{r0}{}')$ of the reference point in the barycentric coordinate system. Equation (8) is obtained when $(\Delta p_x^{r0}{}', \Delta p_z^{r0}{}')$ only have random errors:

$$\left.\begin{aligned} \Delta p_x^{r0}{}' &= a_x x^r{}' + b_x z^r{}' \\ \Delta p_z^{r0}{}' &= a_z x^r{}' + b_z z^r{}' \end{aligned}\right\} \quad (8)$$

Based on the error equation of (8), we obtain the parallax coefficients (a_x, b_x) and (a_z, b_z) of the image point in the X- and Z-direction, respectively. Then, we obtain the systematic errors of the deformation points:

$$\left.\begin{aligned} \Delta p_x^{d0}{}' &= a_x x^d{}' + b_x z^d{}' \\ \Delta p_z^{d0}{}' &= a_z x^d{}' + b_z z^d{}' \end{aligned}\right\} \quad (9)$$

where (x^d', z^d') and $(\Delta p_x^{d0}', \Delta p_z^{d0}')$ are the coordinates and the systematic error of the deformation point in the barycentric coordinate system, respectively.

Then, the corrected parallaxes of the corresponding deformation points are obtained:

$$\left.\begin{aligned} c\Delta p_x^d' &= \Delta p_x^d' - \Delta p_x^{d0}' \\ c\Delta p_z^d' &= \Delta p_z^d' - \Delta p_z^{d0}' \end{aligned}\right\} \quad (10)$$

where $(c\Delta p_x^d', c\Delta p_z^d')$ are the corrected parallaxes of the deformation points in the barycentric coordinate system.

Then, we obtain the corrected displacements of the deformation points based on the reference plane:

$$\left.\begin{aligned} c\Delta x^d &= m \cdot c\Delta p_x^d' \\ c\Delta z^d &= m \cdot c\Delta p_z^d' \end{aligned}\right\} \quad (11)$$

where $(c\Delta x^d, c\Delta z^d)$ are the corrected displacements of the deformation points based on the reference plane

Based on the photograph scale transformation principle [18], we obtain the real displacements on the object plane of a deformation point:

$$\left.\begin{aligned} \Delta x_{pst}^d &= \Delta pstc \cdot c\Delta x^d \\ \Delta z_{pst}^d &= \Delta pstc \cdot c\Delta z^d \end{aligned}\right\} \quad (12)$$

where Δx_{pst}^d and Δz_{pst}^d are the real displacements on the object plane of a deformation point, and $\Delta pstc$ is the coefficient of the photograph scale transformation

Note that the PST-IM-MP method is the IM-MP method when $\Delta pstc$ is equal to 1.

SHUTTLE STEEL SHELF TESTS

Test process

Figure 3 shows the test field of the steel shelf. Before the test, the camera was set 5m from the steel shelf and was levelled. Moreover, we adjusted the camera parameters (focal length 35mm) and turned on the flash to obtain a clear image. Deformation points labelled U0-U5 were set on the columns of the steel shelf where monitoring was needed. The reference system should not be influenced by the shuttles. Therefore, we selected another small steel shelf and set reference points labelled C0-C5 on the shelf to form the reference system. Furthermore, the direction photographed was perpendicular to the reference system and the columns of steel shelf. In addition, the shuttles labelled S1-S3 were mounted on the corresponding tracks. For convenience, we define the direction photographed as north (in Figure 3 (b)).

Note that in the test the reference plane is very close to the object plane. The deformation points and the reference points can be considered to be on the same plane. Thus, in this paper, $\Delta pstc$ is approximately equal to 1.

The testing process is detailed as follows: First, before the shuttles moved the SONY350 camera was used to photograph the steel shelf as a zero image (the reference image).

Second, the camera was used to photograph the steel shelf in successive images when the shuttles S2 and S3 began to move, accelerated, moved at constant speed, decelerated and stopped from the south to the north.

Third, the camera was used to photograph the steel shelf in successive images when the shuttles S2 and S3 began to move, accelerated, moved at constant speed, decelerated and stopped from the north to the south.

Last, thirteen successive images were obtained. In this paper, we define photographing the steel shelf one time as one test. Thus, we completed thirteen tests and obtained the relative deformation of the steel shelf in operation thirteen times.

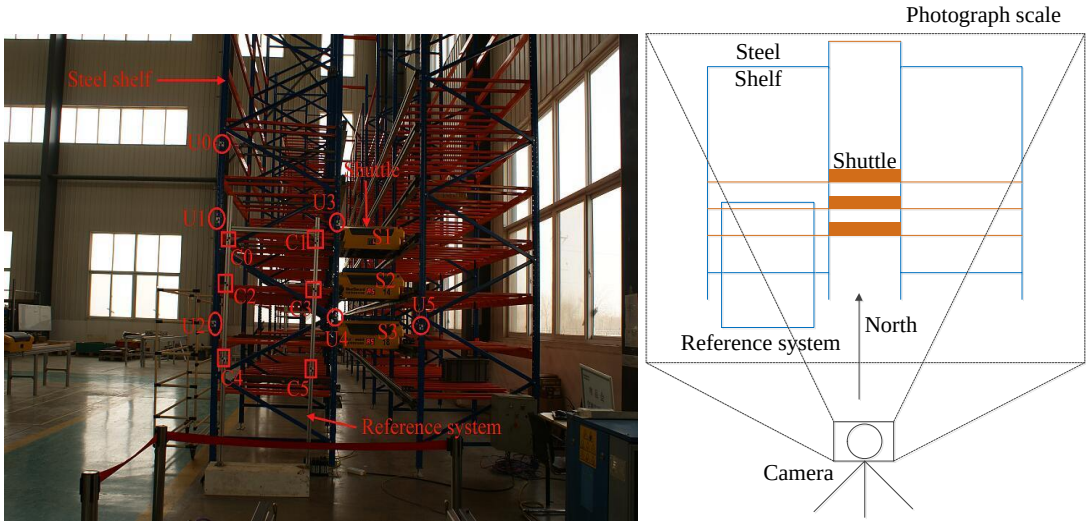

(a) Front view of the test field (taken by Yongqian Zhao)

(b) Relative positions of the camera and steel shelf

Fig. 3 - Test field of the steel shelf

Test results and analysis

In the tests, the pixel displacements of the reference points were zero in theory. However, the pixel displacements of the reference points were not zero in the PST-IM-MP method. As such, these values were considered to be the measurement accuracies of the PST-IM-MP method.

Through data processing, the measurement accuracy of the PST-IM-MP method (Table 4) and deformation values of the deformation points (Table 5) were obtained. In Table 4, |X| represents the absolute value of the measurement accuracy in the X-direction, |Z| represents the absolute value of measurement accuracy in the Z-direction, and CD represents the absolute value of measurement accuracy in the comprehensive direction. The measurement accuracy of

the PST-IM-MP method reaches the sub-pixel level. The maximum and minimum average measurement errors are 0.63 pixels and 0.10 pixels in the X-direction, respectively, 0.37 pixels and 0.28 pixels in the Z-direction, respectively, 0.74 pixels and 0.34 pixels in the comprehensive direction, respectively. The photograph scale is 1.11mm/pixel in the reference system. Note that in this paper, we use the pixel displacements of all six reference points to reflect the measurement accuracy of the PST-IM-MP method. In consideration of space in the civil engineering journal of publication, only a selection of data are shown in Table 4.

In Table 5, the positive and negative X represent the deformation points moving right and left, respectively. The positive and negative Z represent the deformation points moving up and down, respectively. To study visually the stability of the shuttle steel shelves, the deformation trends (Figure 4) were depicted by DPS. Figure 4 clearly shows the maximum deformation, the minimum deformation and the movement trajectory of each deformation point in the X-, Z- and comprehensive directions. Moreover, the deformations of U0-U5 are elastic, and within the allowed deviation (10mm) [19]. These results suggest that the steel shelves are safe.

Tab. 4 - Measurement accuracies/pixel

Test	C0			C1			C2			C3		
	|X|	|Z|	CD	|X|	|Z|	CD	|X|	|Z|	CD	|X|	|Z|	CD
1	0.51	0.02	0.51	0.2	0.77	0.80	0.37	0.37	0.52	0.04	0.04	0.06
2	0.52	0.23	0.57	0.21	0.22	0.30	0.37	0.33	0.50	0.04	0.33	0.33
3	0.99	0.22	1.01	0.01	0.3	0.30	0.01	0.41	0.41	0.00	0.24	0.24
4	0.52	0.59	0.79	0.21	0.77	0.80	0.37	0.55	0.66	0.04	0.87	0.87
5	0.52	0.12	0.53	0.21	0.93	0.95	0.37	0.12	0.39	0.03	0.20	0.20
6	0.99	0.12	1.00	0.01	0.06	0.06	0.01	0.12	0.12	0.00	0.20	0.20
7	0.51	0.88	1.02	0.21	0.93	0.95	0.37	0.12	0.39	0.03	0.20	0.20
8	0.42	0.49	0.65	0.42	0.02	0.42	0.37	0.74	0.83	0.38	0.08	0.39
9	0.62	0.01	0.62	0.03	0.23	0.23	0.33	0.37	0.50	0.01	0.04	0.04
10	0.52	0.12	0.53	0.21	0.01	0.21	0.37	0.08	0.38	0.03	0.08	0.09
11	0.99	0.22	1.01	0.01	0.3	0.30	0.01	0.58	0.58	0.00	0.24	0.24
12	0.13	0.12	0.18	0.13	0.06	0.14	0.3	0.12	0.32	0.70	0.20	0.73
13	0.99	0.59	1.15	0.01	0.22	0.22	0.01	0.45	0.45	0.00	0.87	0.87
Avera	0.63	0.29	0.74	0.14	0.37	0.44	0.25	0.34	0.47	0.10	0.28	0.34

Tab. 5- Pixel displacements of U0-U5/pixel

Test	U0		U1		U2		U3		U4		U5	
	X	Z	X	Z	X	Z	X	Z	X	Z	X	Z
1	0.24	0.58	0.00	1.33	-1.35	0.06	1.49	-0.43	0.08	-0.06	-0.13	-0.57
2	1.24	1.10	0.00	0.57	-0.36	-0.09	1.49	1.26	0.08	0.30	0.86	0.09
3	0.46	0.88	-0.50	0.97	-0.50	1.15	1.06	0.62	-0.04	0.42	0.12	0.25
4	0.36	0.44	-0.86	0.78	-1.23	1.29	0.26	-0.04	-0.18	0.05	-0.35	0.56
5	1.35	-0.36	0.13	0.05	-1.23	0.66	1.26	0.22	-0.18	-0.60	-0.35	-0.08
6	-0.53	0.64	-0.50	0.05	-1.49	0.66	0.06	0.22	-0.04	0.39	0.12	-0.08
7	1.35	0.64	0.13	0.05	-0.24	0.66	1.26	0.22	-0.18	-0.60	-0.35	-0.08
8	-0.52	0.68	-1.15	0.71	-0.70	-0.2	0.38	1.35	-0.31	0.08	-0.13	-0.10
9	-1.00	1.58	-0.92	1.33	-1.85	0.06	1.08	0.56	0.05	-0.06	0.53	-0.57
10	1.46	1.33	0.25	0.41	-0.11	0.56	0.03	0.16	-1.43	-1.08	-1.56	-0.90
11	-0.53	1.99	-0.50	1.10	-0.50	1.27	1.06	-0.6	-0.04	0.16	0.11	-0.97
12	-0.72	0.64	-1.41	1.05	-1.06	0.66	0.12	0.22	-0.66	0.39	0.51	-0.08
13	-0.53	0.44	-0.50	0.78	-0.50	0.30	1.06	0.95	-0.04	0.05	0.12	-0.43

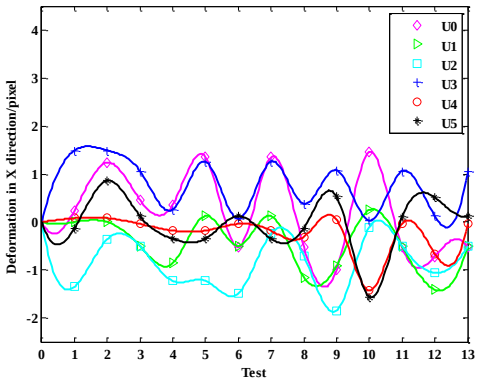

(a)deformation in the X-direction

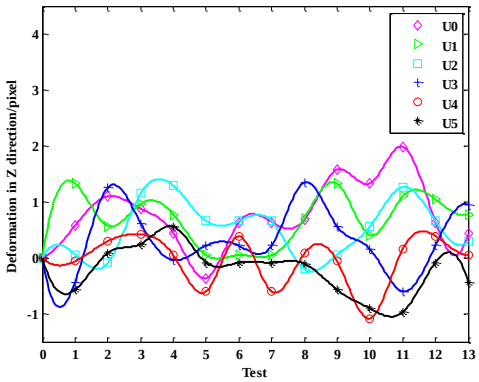

(b) deformation in the Z-direction

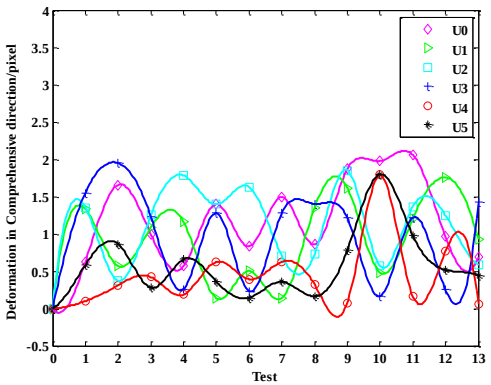

(c) deformation in the comprehensive direction

Fig. 4 - Deformation trends of the shuttle steel shelves

As the maximum deformation is the key to study the stability of the steel shelf, we analyse the maximum deformations of U0-U5 in the X-, Z- and comprehensive directions: U0 moved

right 1.46 pixels in test 10, up 1.99 pixels in test 11, and 2.06 pixels in the comprehensive direction in test 11. U1 moved left 1.41 pixels in test 12, up 1.33 pixels in tests 1 and 9, and 1.76 pixels in the comprehensive direction in test 12. U2 moved left 1.85 pixels in test 9, up 1.29 pixels in test 4, and 1.85 pixels in the comprehensive direction in test 9. U3 moved right 1.49 pixels in tests 1 and 2, up 1.35 pixels in test 8, and 1.95 pixels in the comprehensive direction in test 2. U4 moved left 1.43 pixels, down 1.08 pixels, and 1.79 pixels in the comprehensive direction in test 10. U5 moved left 1.56 pixels in test 10, down 0.97 pixels in test 11, and 1.80 pixels in the comprehensive direction in test 10.

Thus, it is necessary to further analyse the operation situations of the shuttle steel shelves in tests 1, 2, 4, 8, 9, 10, 11 and 12. Figure 3 shows the locations of the deformation points on the columns before (the red circles) and after (the blue asterisks) the tests. The changes in the locations of deformation points directly reflect the operational situations of the steel shelves. In Figure 3, the red lines represent the original locations of the columns. The blue curves represent the locations of the corresponding columns after the tests. The arrows represent the movement directions of the deformation points. The distances between the columns and the lengths of the column decrease by certain proportions.

Figure 5 (a) shows the changes in the locations of the deformation points when the shuttles began to move from the south side. Strong tensile stress developed between column 1 and column 2 because U2 moved left 1.35 pixels and U3 moved right 1.49 pixels. Strong shear stress developed between U1 and U2 because U2 moved left 1.35 pixels and U1 remained in the same location.

Figure 5 (b) shows the changes in the locations of the deformation points when the shuttles accelerated from the south to the north. Strong shear stress developed between U0 and U1 because U0 moved right 1.24 pixels and U1 remained in the same location. Strong tensile stress developed between column 1 and column 2 because U1 remained in the same location and U3 moved right 1.49 pixels. Strong tensile stress developed between column 2 and column 3 because U4 moved right 0.08 pixels and U5 moved right 0.86 pixels.

Figure 5 (c), (d) and (e) shows the changes in the locations of the deformation points when the shuttles decelerated from the south to the north, accelerated from the north to the south and moved at constant speed from the north to the south, respectively. Strong tensile stresses also developed between column1 and column2 in these tests.

Figure 5 (f) shows the changes in the locations of the deformation points at the moment when the shuttles decelerated from the north to the south. Strong shear stress developed between U0 and U1. Strong compressive stress developed between column 1 and column 2 due to U4 moving left 1.43 pixels and U3 moving right 0.03 pixels. Moreover, U4 and U5 were more stable than the other deformation points because these points were on the bottom of the shuttle steel shelves. However, U4 and U5 developed more deformation in test 10 when the shuttle decelerated from the north to the south. U4 and U5 moved down 1.08 pixels and 0.97 pixels, respectively. These points also moved left 1.43 pixels and 1.56 pixels, respectively. These results suggests that the bottoms of the shuttle steel shelves bear high impacts when the shuttle decelerates. In turn, deceleration makes the top left corner of the shuttle steel shelves wobble strongly, such as U0 moving right 1.46 pixels and up 1.33 pixels.

Figure 5 (g) and (h) shows the changes in the locations of the deformation points when the shuttles decelerated from the north to the south. Strong tensile stresses developed between column 1 and column 2 in tests 11 and 12. In test 12, tensile stress developed between column 2 and column 3.

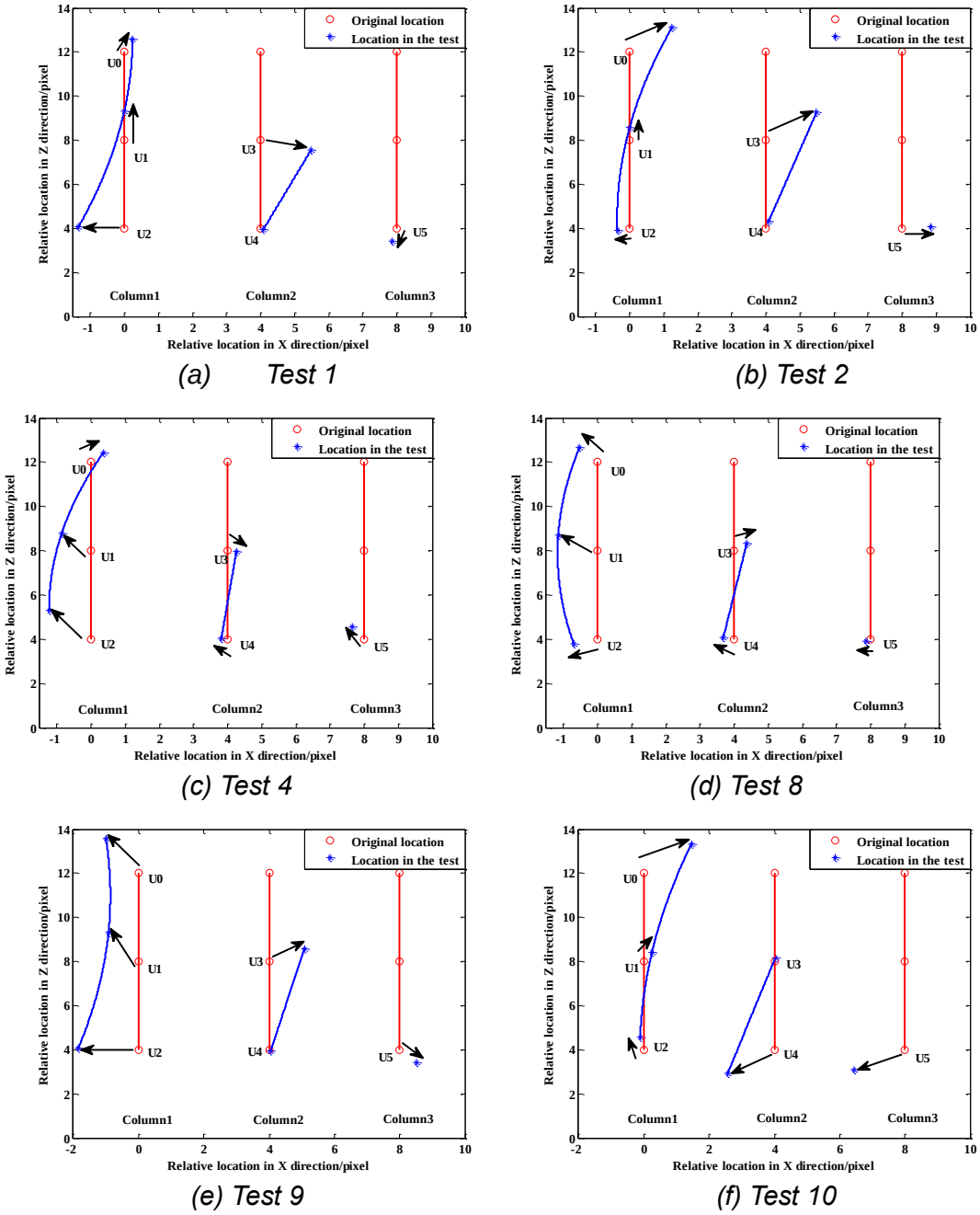

(a) Test 1 (b) Test 2

(c) Test 4 (d) Test 8

(e) Test 9 (f) Test 10

Fig. 5 - Changes in the locations of the deformation points

DOI 10.14311/CEJ.2019.02.0012

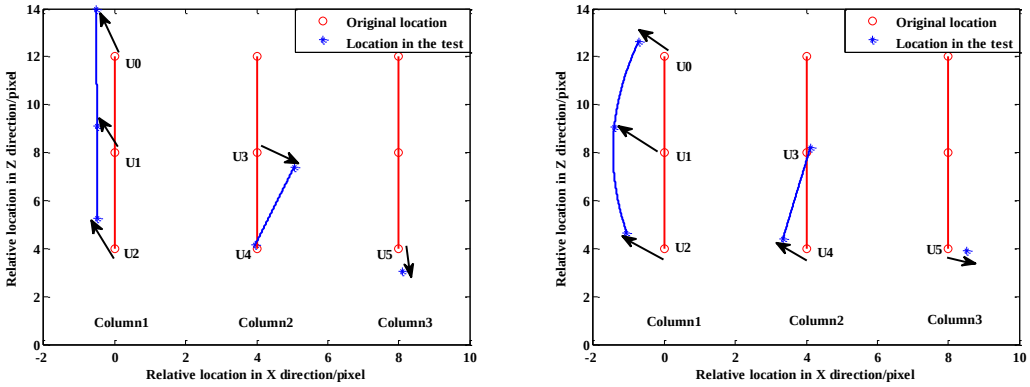

(g) Test 11 *(h) Test 12*

Fig. 5 - Changes in the locations of the deformation points

In conclusion, the stresses on the shelves are complicated when the shuttles are in operation. The beams between the columns bear the tension and shear caused by the shuttle movement, which is different from traditional steel shelves. If the shelves were full and the components were in extreme equilibrium, the tension and shear caused by the shuttle movement would cause the beams to yield and result in damage to the steel shelf or even in collapse. Moreover, only two shuttles were in operation in the test. The stresses on the shelves would be more complicated if the shuttle steel shelves were normally used as multiple shuttles would be in operation. Thus, a DPS can be used to monitor the safety of shuttle steel shelves and depict their deformation trends in real time. A DPS can warn of possible dangers and mitigate hazards based on these real-time deformation trends. Furthermore, the data from the DPS in this study can be used to study the stability of shuttle steel shelves to improve the stability of their design.

CONCLUSION

This study used a DPS (digital photography system) to monitor the dynamic deformation of shuttle steel shelves to warn of possible dangers and mitigate hazards when the shuttles were in operation. The PST-IM-MP (photograph scale transformation-image matching-motion parallax) method was used to process these images over time. The stresses in the shuttle steel shelves were analysed based on the data. The conclusions from the study are the following:

(1) The measurement accuracy of the PST-IM-MP method reaches the sub-pixel level because the maximum and minimum measurement errors are 0.63 pixels and 0.10 pixels in the X-direction, respectively, 0.37 pixels and 0.28 pixels in the Z-direction, respectively, and 0.74 pixels and 0.34 pixels in the comprehensive direction, respectively.

(2) The beams between the columns bear the tension and shear stresses caused by the shuttle movement, which differs from the response of traditional steel shelves.

(3) The top left of the shuttle steel shelf wobbles more than other positions when the shuttles are in operation.

(4) The bottoms of the shuttle steel shelves bears high impacts when the shuttles decelerate. In turn, deceleration makes the top left corner of the steel shelf wobble strongly.

(5) The shuttle steel shelves are robust as the deformations of the shelves are elastic and within the allowed10mm.

(6) The DPS in this study can monitor dynamic deformations of shuttle steel shelves in real time to warn of possible dangers and mitigate hazards.

As the dynamic deformation data of shuttle steel shelves in operation is of great importance in the safety related to the shelves, it is essential to use a DPS to monitor the dynamic deformation of the shuttle steel shelves during operation. The DPS can process the images and depict the deformation trends over time, which can be used to warn of possible dangers on site and mitigate hazards. Thus, DPS will be popular in monitoring the safety of shuttle steel shelves in operation in the future and will provide data support to improve the stability design of shuttle steel shelves.

ACKNOWLEDGMENTS

This study was supported by Postgraduate Research & Practice Innovation Program of Jiangsu Province (Grant No.: KYCX19_2162)，the National Key Research and Development Program (2018YFC0604704), the Science and Technology Project of the Shandong Province of China (Grant No. 2010GZX20125), PhD research fund project of Shandong Jianzhu University, 2016 (Grant No. XNBS1635) and the Science and Technology Project of Shandong's Department of Housing and Urban-rural Construction (Grant No. 2017-K2-001). The funders Chengxin Yu and Yongqian Zhao were involved in the writing, editing, and approval of the manuscript and decision to publish this paper.

REFERENCES

[1] Yu CX, Ding XH, Chen MZ, Xiao P (2013) The Application of Digital Cameras in Monitoring Dynamic Deformation of Steel Shelf. Applied Mechanics & Materials 405-408:873-877
[2] Kwon YB, Hancock GJ (1992) Tests of Cold-Formed Channels with Local and Distortional Buckling. Journal of Structural Engineering 118 (7):1786-1803
[3] Chen B, Yin ZJ, Yang J, Wang CY (2011) Integration Research for Steel Shelf CAD/CAE Calculation and Analysis System. Advanced Materials Research 243-249:6154-6158
[4] Gilbert BP, Rasmussen KJR (2011) Determination of the base plate stiffness and strength of steel storage racks. Journal of Constructional Steel Research 67 (6):1031-1041
[5] Aguirre C (2005) Seismic behavior of rack structures. Journal of Constructional Steel Research 61 (5):607-624
[6] White DW, Hajjar JF (1997) Accuracy and simplicity of alternative procedures for stability design of steel frames. Journal of Constructional Steel Research 42 (3):209-261
[7] Tian Qiu (2016) Analysis of the loading capacity and seismic resistance and the motion of the shuttle bus of automated warehouse. Master' thesis, Kunming University of Science and Technology. (in Chinese)
[8] Yongqian Zhao (2016) Research on the stability and deformation monitoring of the dense channels accessing-sorting racks system. PhD thesis, Shandong University. (in Chinese)
[9] Lovse JW, Teskey WF, Lachapelle G, Cannon ME (1995) Dynamic Deformation Monitoring of Tall Structure Using GPS Technology. Journal of Surveying Engineering 121 (1):35-40
[10] Ma DL, Cui J, Wang SY (2014) Application and Research of 3D Laser Scanning Technology in Steel Structure Installation and Deformation Monitoring. Applied Mechanics & Materials 580-583:2838-2841
[11] Ghorbani R, Matta F, Sutton MA (2015) Full-Field Deformation Measurement and Crack Mapping on Confined Masonry Walls Using Digital Image Correlation. Experimental Mechanics 55 (1):227-243
[12] Jiang R, Jauregui DV (2010) Development of a digital close-range photogrammetric bridge deflection measurement system. Measurement 43 (10):1431-1438
[13] Yu CX, Xia X, Qin FH, Xiao P (2014) The Application of Digital Photography Techniques in

Structure Deformation Measurement. Applied Mechanics & Materials 475-476:204-208
[14] Yanagi H, Chikatsu H (2012) Factors and Estimation of Accuracy in Digital Close Range Photogrammetry using Digital Cameras. Journal of the Japan Society of Photogrammetry 50 (1):4-17
[15] Zhang G, Guo G, Li L, Yu C (2018) Study on the dynamic properties of a suspended bridge using monocular digital photography to monitor the bridge dynamic deformation. Journal of Civil Structural Health Monitoring 8 (2):1-13
[16] Zhang G, Guo G, Yu C, Li L (2018) Monitoring dynamic global deflection of a bridge by monocular digital photography. Civil Engineering Journal 27 (2):168-182. doi:10.14311/CEJ.2018.02.0014
[17] Shapiro, R. (1978). Direct linear transformation method for three-dimensional cinematography. Res. Quart. 49, 197-205.
[18] Zhang G, Guo G, Yu C, Li L, Hu S, Wang X (2018) Monitoring Instantaneous Dynamic Displacements of Masonry Walls in Seismic Oscillation Outdoors by Monocular Digital Photography. Mathematical Problems in Engineering 2018. doi:10.1155/2018/4316087
[19] Institute RM (2012) Specification for the Design, Testing, and Utilization of Industrial Steel Storage Racks. Springer Netherlands.